

TEM INVESTIGATION OF METALLIC MATERIALS – AN ADVANCED TECHNIQUE IN MATERIALS SCIENCE AND METALLURGY

PREISKAVE KOVINSKIH MATERIALOV S PRESEVNO ELEKTRONSKO MIKROSKOPIJO - MODERNA TEHNIKA V ZNANOSTI O MATERIALIH IN METALURGIJI

Darja Jenko

Institute of Metals and Technology, Lepi pot 11, p. p. 431, SI-1000 Ljubljana, Slovenia
darja.jenko@imt.si

Prejem rokopisa – received: 2011-04-21; sprejem za objavo – accepted for publication: 2011-07-07

The investigation of different metallic materials using high-resolution transmission electron microscopy (HRTEM) is presented. After thinning using argon ion-slicing thin foil specimens were prepared and further analyzed by various TEM analysing techniques at 200 kV, that make a powerful combination to resolve a large number of problems encountered in materials science and metallurgy. Some case studies of such problems are presented: influence of foaming agents in manufacturing processes of aluminium metal foams, removal of remaining oxides from the surface of duplex stainless steel (DSS), effect of low temperature ageing on properties of DSS, effect of heat treatment on the microstructure and properties of precipitate containing aluminium alloys.

Key words: transmission electron microscopy, Ar ion slicing, silicon, duplex stainless steel, aluminium alloy

V prispevku so opisane preiskave različnih kovinskih materialov z visokoločljivostno presevno elektronsko mikroskopijo. Vzorce tankih folij smo po tanjšanju z rezanjem z ioni argona nadalje preiskovali pri 200 kV z različnimi analiznimi tehnikami presevne elektronske mikroskopije, ki so močna kombinacija pri reševanju velikega števila problemov, s katerimi se srečujemo v znanosti o materialih in metalurgiji. Predstavljenih je nekaj primerov takšnih problemov: vpliv penilnih sredstev v proizvodnji kovinskih aluminijevih pen, odstranitev preostalih oksidov s površine dupleksnega nerjavnega jekla (DSS), vpliv nizkotemperaturnega staranja na lastnosti DSS, vpliv toplotne obdelave na mikrostrukturo in lastnosti aluminijevih zlitin z vključki.

Ključne besede: presevna elektronska mikroskopija, rezanje z ioni Ar, silicij, dupleksno nerjavno jeklo, aluminijeva zlitina

1 INTRODUCTION

Today electron microscopy, more specifically transmission electron microscopy (TEM) is indispensable for the characterization of various materials mainly on nanometer (atomic) scale. Nanotechnology is the understanding and control of matter at dimensions between approximately 1 nm and 100 nm, where unique phenomena enable novel applications.¹ The encompassing nanoscale science, engineering, and technology, nanotechnology involves imaging, measuring, modeling, and manipulating matter at this size scale. 'Imaging, measuring, modeling, and manipulating matter' can be accomplished using TEM. By means of TEM measurements information is obtained on crystal lattice, cell parameters, different phases, grain size, morphology, density of defects (dislocations, stacking faults, twins) etc.

The word microscope is derived from Greek mikros (small) and skopein (to look, to see). From the dawn of science there has been an interest in being able to look ever smaller details of the world around us. Materials scientists wanted to see inhomogeneities and imperfections in ceramics², glasses, polymers, semiconductors, crystals (single, liquid)³, metals, alloys, steels^{4,5}, com-

posite mixtures of these materials, and different powder mixtures⁶, with sporadic observations of wood, textiles, and concrete. Biologist wanted to examine the structure of cells, bacteria, viruses, and colloidal particles. In geology, the detailed study of rocks, minerals, and fossils on a microscopic scale provides insight into the origins of our planet and its valuable mineral resources. Because of today's better analysing techniques, including TEM, it is possible to investigate all these materials from different fields of science in more exact and detailed manner using TEM or using other analytical techniques in combination with TEM. In the research program of the institute several research works for instance on surface reactions and processes⁷⁻²², creep resistant steels properties and microstructure²³, effect of low temperature ageing on properties of Fe-NiCrMo alloys^{24,25} were included in a number of reports prepared and of work published would certain be of better quality if TEM was used also and the examination or conclusion strengthened by TEM analyses.

Given sufficient light, the unaided healthy human eye can distinguish two points 0.1–0.2 mm apart.²⁶ If the points are closer together, they will appear as a single point. This distance is called the resolving power or

resolution of the eye. A lense or an assembly of lenses (a microscope) can be used to magnify this distance and enable the eye to see points even closer together than 0.1 mm.

Most microscopes can be classified as one of three basic types: 1. optical or light, which use visible light and transparent lenses to see objects as small as about 1 μm , 2. charged particles (electron and ion), which use a beam of charged particles instead of light and electromagnetic or electrostatic lenses to see the particles, or 3. scanning probe, which use a physical probe (a very small, very sharp needle) that scans over the specimen in contact or near-contact with the surface.^{26,27} Both latter types of microscopes, charged particles and scanning probe are capable of atomic scale resolution.

In the 1920s, it was discovered that accelerated electrons behave much like light in vacuum.²⁶ They travel in straight lines and have wave-like properties, with a wavelength that is about 100 000-times shorter than that of visible light. E. Ruska at the Technical College in Berlin, under the tutelage of M. Knoll, combined these characteristics and built the first transmission electron microscope (TEM) in the early 1930s. This first TEM used two magnetic lenses, and three years later he added a third lens and demonstrated a resolution of 100 nm, twice as good as that of the light microscope (a modern visible-light microscope has a magnification of about 1 000-times and enables the eye to resolve objects separated by 200 nm).

L. de Broglie's famous equation²⁶ shows that the wavelength λ in nm of electrons is related to their energy E/eV and, if we ignore relativistic effects, we can show approximately that (ignoring the inconsistency in units)

$$\lambda = 1.22/(E^{1/2}) \quad (1)$$

We can calculate from equation (1) that by 100 keV electron, λ is ≈ 4 pm (0.004 nm), which is much smaller than the diameter of an atom.

The resolving power of a TEM is determined by a combination of beam voltage, aperture size and lense aberrations.²⁶ Today, TEMs have reached resolutions better than 0.05 nm, more than $4 \cdot 10^3$ -times better than a typical visible-light microscope and $4 \cdot 10^6$ -times better than the unaided eye.

Despite the advantages of the TEM there are some drawbacks.²⁶ First of all, the price to pay for high-resolution imaging technique is that at one time we only look at small part of our specimen. So we have an instrument that is not a good sampling tool. Another problem is that the TEM presents us with 2D images of 3D specimens, viewed in transmission. So we have to be aware of the artifacts which abound in TEM images and be cautious in their interpretation. Also a detrimental effect of ionization is that it can damage our specimen. And there is always a possible danger of exposing oneself to ionizing radiation although modern TEMs are remarkably well engineered and designed with safety as a primary concern. A major limitation of the TEM is we need thin

(electron transparent) specimens. Generally, specimens <100 nm should be used wherever possible. For high-resolution (HR) TEM imaging or electron spectrometry, specimen thicknesses <50 nm (even <10 nm) are essential. This requirement is a function of the electron energy and the average atomic number (Z) of our specimen. The thinning processes that we use do affect the specimens, changing both their structure and chemistry. So we need to be aware of the drawbacks of specimen preparation and learn to recognize the artifacts introduced by standard preparation methods.^{26,28,29}

In the Institute of Metals and Technology (IMT) in Ljubljana, Slovenia, the JEOL JEM-2100 TEM (**Figure 1**) started to operate in December 2008 and it was finally installed in March 2009. It is a high-resolution (HR) and analytical electron microscope (AEM) that not only offers TEM images and diffraction patterns, but also incorporates a computer control system which integrates a scanning transmission electron microscope (STEM) image observation device with bright-field (BF) and dark-field (DF) detectors, as well as an energy dispersive X-ray spectrometer (EDXS) JED-2300T. The microscope operates at magnification ranges from 50-times to $1.5 \cdot 10^6$ -times in TEM mode. High stability of the high

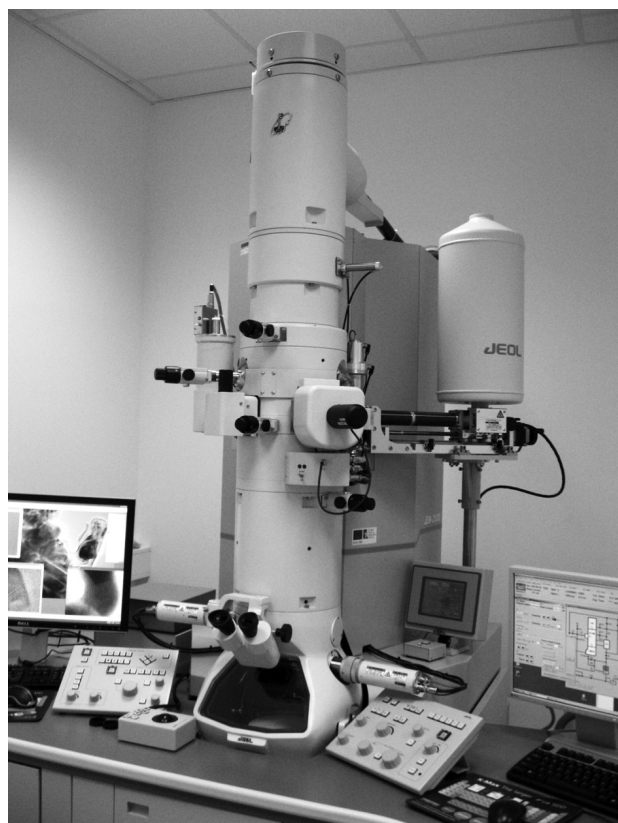


Figure 1: JEOL JEM-2100 high-resolution and an analytical electron microscope equipped with STEM unit (bright- and dark-field detectors) and EDXS detector

Slika 1: JEOL JEM-2100, visokoločljivostni in analitski elektronski mikroskop, opremljen z enoto STEM (z detektorjem za opazovanje v svetlem in temnem polju) in detektorjem EDXS

voltage and beam current achieves a high resolution of 0.23 nm (point resolution) and 0.14 nm (lattice resolution) at 200 kV (with a high brightness LaB₆ electron source). The accelerating voltage in the range of 80 kV and 200 kV can be changed easily. An optimum accelerated voltage can be selected quickly to observe beam-sensitive materials such as biological materials, polymers or carbon nanotubes. For imaging Gatan ORIUS CCD camera with Gatan Digital Micrograph software is used. It is also possible to heat the specimens up to 1000 °C (maximum to 1100 °C for 48 h).

In this article our experience in use of JEOL JEM-2100 electron microscope is presented as multi-disciplinary instrument providing services for investigations in the microfield and nanofield encompassing wide variety of topics. Performance of the microscope is demonstrated with some results showing its contribution to our studies of nano-materials.

2 EXPERIMENTAL WORK

All the specimens of thin foils, except gold particles, used for TEM investigations were prepared using argon ion-slicing with JEOL EM-09100IS Ion Slicer. The Ion Slicer partly thins the specimen. It is possible to prepare cross-section or plan-view thin foil specimens. The instrument irradiates an argon ion beam on the specimen, which is partially masked with a shield belt. The instrument consists of a specimen chamber, which is evacuated with a turbo-molecular pump, ion source tilt mechanism, mask-belt retainer, specimen stage mechanism, camera and other parts. Preparation of thin foils by means of argon ion slicing using Ion Slicer is a novel method that enables a quick preparation of high quality specimens for TEM. It is suitable for the preparation of different speci-

mens for TEM, not only metals, and therefore useful in different fields of science and industry.

Specimens for TEM, thicknesses of around 500 µm, were cut out of a bulk material in rectangular area of 0.5–1.0 mm × 2.8 mm (bulk cross-section preparation). They were thinned to less than 100 µm with JEOL Handy Lap (in many cases with grinding paper SiC 800 only, with the grain size around 22 µm), mounted on an Ion Slicer specimen holder, partially masked with a shield belt (bulk cross-section preparation) and further thinned with an argon ion beam. The parameters of thinning depended on the type of the specimen. The slicing process started at the pressure of 10⁻⁵ Pa or 10⁻⁴ Pa and alternated between the front and the backside of the specimens while they were rotating. The beam was tilted between 1.0° to 2.5°. Accelerating voltage between 4.0 kV and 6 kV, argon gas flow rate between 7.1 and 7.5 (arbitrary units) and side change interval of 30 s or 60 s were chosen. After a large thin area of the specimens up to 300–500 µm × 700 µm was obtained, a small hole was generated in the thinnest region of the specimens. Polishing was used with a tilt angle of 0.5°, at the accelerating voltage of 2 kV and side change interval of 15 s or 40 s for 7 min, 10 min or 15 min. As an example, the total time of slicing was 3 h and 48 min for Si, 6 h and 43 min for AA7075 aluminium alloy and up to 9 h and 40 min for duplex stainless steels (DSS).

Optical microscope image as an example of thin section specimen of silicon after using argon ion-slicing is shown in **Figure 2**. We can see that large thin electron transparent areas are still surrounded by thick specimen parts which enhance the stability of the specimens. After argon ion-slicing the specimens were examined with TEM at 200 kV using conventional TEM (CTEM), HRTEM, electron diffraction, EDXS, and STEM (in this article the results of STEM using BF detector, EDXS mapping, and line profile are presented).

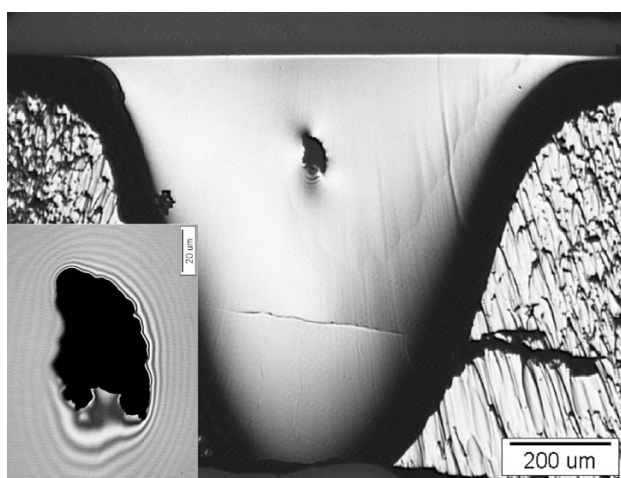


Figure 2: Optical microscope image of thin section specimen of silicon for TEM prepared by argon ion-slicing. Thin electron transparent areas are surrounded by thick sample parts

Slika 2: Posnetek z optičnim mikroskopom vzorca tanke folije silicija po rezanju z ioni argona. Tanka področja, presevana za elektrone, so obdana z debeljšimi deli vzorca

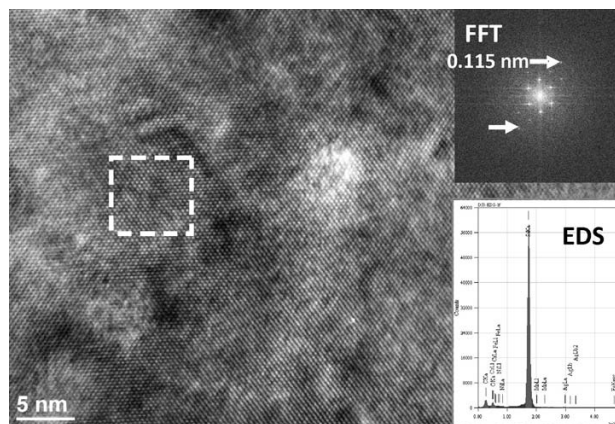


Figure 3: High-resolution (HR) TEM image of silicon specimen. The insets are fast Fourier transform (FFT) of the image part marked by the white dash-lined square, and chemical composition analysis (EDXS)

Slika 3: Visokoločljivostna slika TEM vzorca silicija. Vstavljeni sliki prikazujeta hitro Fourierjevo transformacijo (FFT) dela slike, ki je označena z belim črtnim kvadratom, in kemijsko sestavo (EDXS)

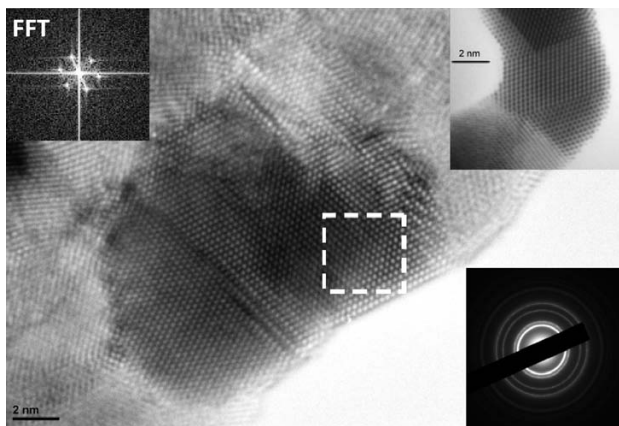


Figure 4: High-resolution (HR) TEM image of gold particles. The insets are detailed HRTEM image at magnification of $1.2 \cdot 10^6$ (1.2 M), fast Fourier transform (FFT) of the image part marked by the white dash-lined square, and diffraction pattern

Slika 4: Visokoločljivostna slika TEM zlatih delcev. Vstavljene slike prikazujejo posnetek HRTEM pri povečavi $1.2 \cdot 10^6$ (1,2 M), hitro Fourierjevo transformacijo (FFT) dela slike, ki je označena z belim črtkanim kvadratom, in uklonski posnetek

3 RESULTS AND DISCUSSION

In the frame of this article it is difficult to refer to the great variety of routine investigations performed at IMT. Instead, some case studies of different applications are presented.

3.1 Verification of performance of TEM/HRTEM/EDXS

Figure 3 shows a HRTEM image of silicon thin foil. The insets are fast Fourier transform (FFT) and chemical composition analysis (EDXS). This was the first specimen prepared to test the performance of JEOL JEM-2100 at IMT. As we could observe in **Figure 2**, the specimen was excellently prepared by thinning with argon ion-slicing. There were many observation areas which were electron transparent, as a matter of fact, the whole foil around the hole was suitable for TEM investigation. Usually, the specimens are covered by a (partly) amorphous surface layer due to preparation damage, which should be kept as thin as possible, as amorphous material decreases the signal-to-noise ratio of the image. In this case, as well in majority of other thin foil specimens, there was no amorphous layer present or it was very thin, a few nm thick.

As follows from the FFT, the lattice fringes with spacing as fine as 0.115 nm could be observed. Such lattice resolution achieved with our instrument appears to be even better than that specified in the official table of the key-features published for JEM-2100 (LaB₆) microscope (lattice resolution 0.14 nm).

Another example is related to HRTEM imaging of gold particles (**Figure 4**). The insets are detailed

HRTEM image at magnification of $1.2 \cdot 10^6$ (1.2 M), FFT and diffraction pattern. Although the microscope is not installed on the ground floor but on the second floor, the performance is excellent.

3.2 Verification of performance of CTEM/HRTEM/STEM/EDXS

Figure 5 and **Figure 6** present, beside CTEM and HRTEM imaging with diffraction pattern of thin foils of aluminium metal foam with closed-cell structure and oxide layers on the surface of duplex stainless steel (DSS), the performance of the microscope in STEM mode which we usually employ with EDXS line scan (**Figure 5**) or elemental mapping (**Figure 6**) to provide information on the chemical composition of very small volumes of material.

3.2.1 Characterization of aluminium metal foam with closed-cell structure

Metal foams are uniform dispersion of a gaseous phase in the solid metal with low densities and novel physical and mechanical properties. Aluminium metal foams with closed-cell structure are manufactured with different foaming agents that are gas releasing substances.^{30–32} Closed-cell structure has high impact energy absorption that is very important mechanical property in several industries. An example of TEM investigation of closed-cell aluminium metal foam thin foil specimen is shown in **Figure 5**. The study was

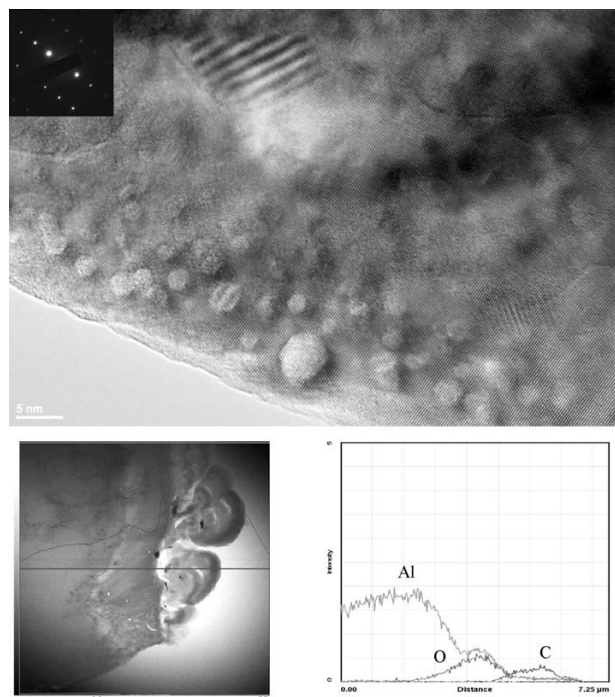


Figure 5: High-resolution (HR)TEM image with diffraction pattern of the aluminium metal foam with closed-cell structure. STEM line profile is also shown

Slika 5: Posnetek HRTEM z uklonsko sliko vzorca kovinske aluminjske pene z zaprto poroznostjo. Prikazan je tudi linijski profil STEM

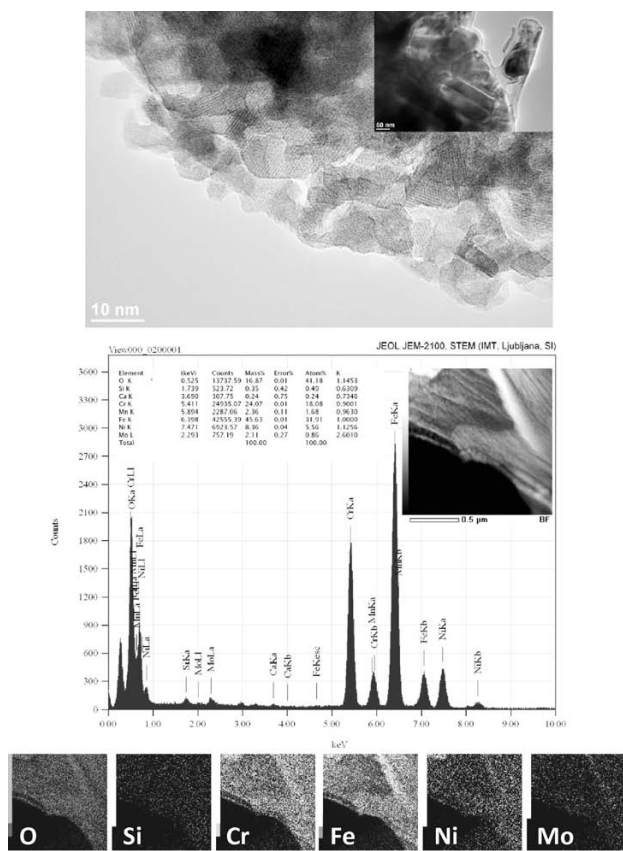


Figure 6: Upper image is high-resolution (HR) TEM image of oxide layer on the surface of duplex stainless steel (DSS, 2205 alloy) specimen. The inset is conventional transmission electron microscopy (CTEM) image. Lower image is chemical analysis (STEM-EDXS) with the inset of bright-field (BF) image and EDXS elemental mapping of DSS specimen

Slika 6: Zgornja slika prikazuje visokoločljivostno sliko TEM oksidne plasti na površini vzorca dupleksnega nerjavnega jekla (DSS, zlitina 2205). Vstavljena slika je posnetek konvencionalne presevalne elektronske mikroskopije (CTEM). Spodnja slika prikazuje kemijsko analizo z rentgensko spektroskopijo (STEM-EDXS) oksidne plasti vzorca DSS z vstavljeno sliko v svetlem polju in ploskovno analizo EDXS

focused on the analysis of cell walls. Detailed characterization of the microstructure was performed on thin section specimens, as for example HRTEM, electron diffraction and STEM. Electron diffraction method was used to carry out the microstructure–crystallographic analysis of phases, STEM BF imaging and EDXS line profiling to determine elemental distribution. At least two oxide layers with different ratios of aluminium and oxygen appeared at the interface aluminium-pore. The ongoing research will clarify the course of reactions. The results of this study may contribute to the development of cheaper manufacturing processes of aluminium foams, and of a wide range of products with core-based aluminium foams as well.

3.2.2 Examination of oxide layers on the surface of duplex stainless steel (DSS, 2205 alloy)

Some of the undesired properties of steel are also degradation and corrosion of stainless steel as result of

not properly cleaned surfaces at the production end. Steel sheet DSS (2205 alloy), thickness of 12 mm, was produced by standard method for thick steel sheets with continuous casting, hot rolling, recrystallization and sandblasting.^{33–35} Scale on the surface may aggravate the properties of stainless steels and disturb the processing of material. Unfortunately, the scale on the surface of sheets is not completely removed with sandblasting. The remainder of oxides was studied by TEM (**Figure 6**). Some high-resolution images of oxides were taken in the thinnest places of the sample and some TEM/EDXS analyses were made in those places. Oxides that form on the surface are mainly Cr_xO_y type. The most common oxide is Cr_2O_3 . Because of heat treatment of the material, some elements like Mn, Fe, Mo, segregated on the surface of steel where oxides are formed. TEM/EDXS analyses and STEM (BF) with EDXS elemental mapping confirmed formation of Cr-, Fe- and Mn-oxides (the latter not shown in STEM-EDXS elemental mapping). Those oxides were also confirmed with X-ray photoelectron spectroscopy (XPS). Results of high-temperature oxide layers on the surface of DSS enabled us to determine the mechanism and kinetics of formation of these oxide layers, which grow at annealing. Furthermore, they enabled us to understand how to optimally and environmentally friendly remove refractory oxide layers from the surface, which is of great importance for the steel producers.

3.2.3 Investigation of isothermal annealing (ageing) of duplex stainless steel (DSS, 258 alloy type)

Thin foils for investigations of DSS (258 alloy type), non-aged and aged (annealed at 300 °C and 350 °C for 10 000 h and 30 000 h), were studied by means of TEM

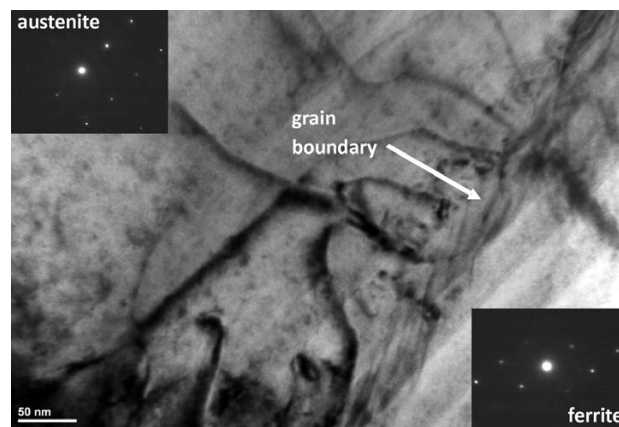


Figure 7: TEM image of accumulation of dislocations at the grain boundary between ferrite and austenite in duplex stainless steel (DSS, 258 type) aged specimen (annealed at 350 °C for 30 000 h). The insets are diffraction patterns of ferrite (bcc – body-centered cubic structure) and austenite (fcc – face-centered cubic structure)

Slika 7: Posnetek TEM kopičenja dislokacij na meji zrn med feritom in avstenitom v staranem (350 °C, 30 000 h) dupleksnem nerjavnem jeklu (DSS, tip 258). Vstavljene slike prikazujeta uklonska posnetka ferita (bcc – telesno centrirana kubična struktura) in avstenita (fcc – ploskovno centrirana kubična struktura)

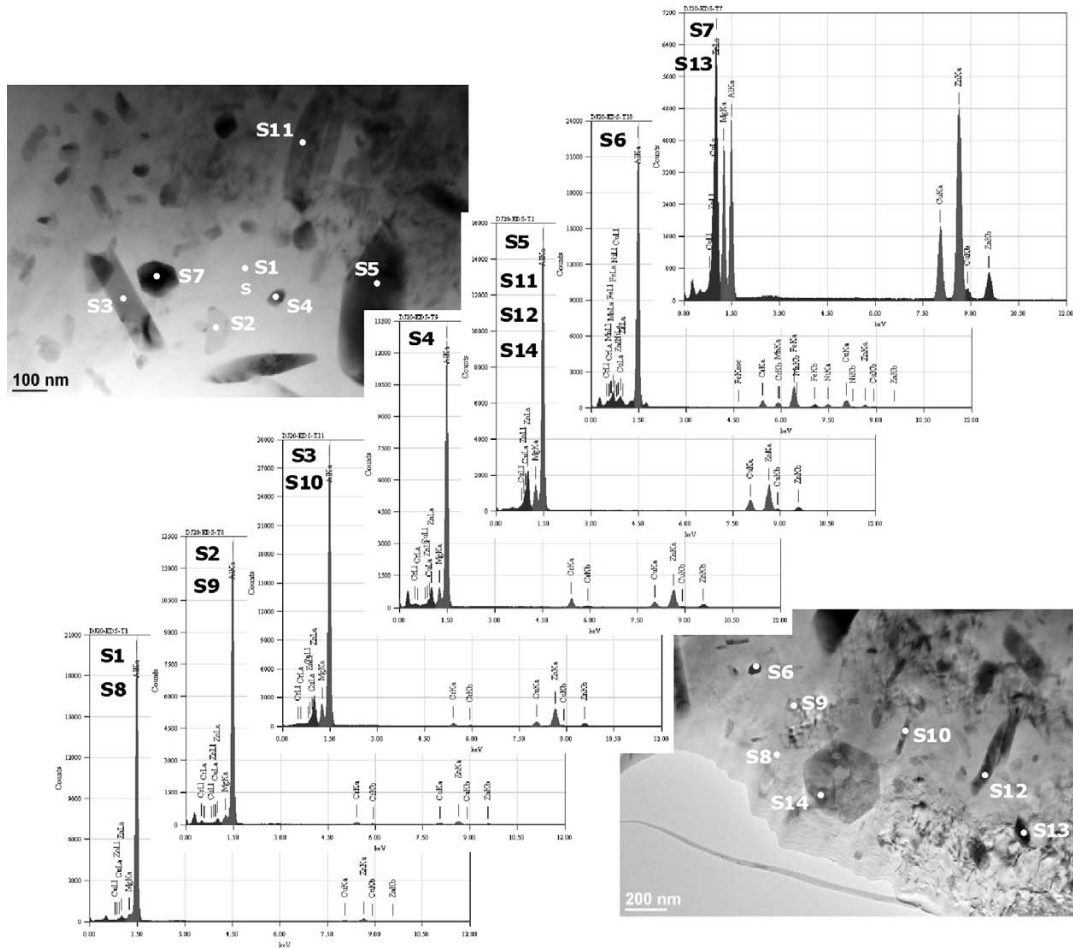


Figure 8: TEM images and chemical composition analyses (EDXS) of precipitates in AA7075 aluminium alloy
Slika 8: Posnetka TEM in analize kemijske sestave (EDXS) vključkov v aluminijevi zlitini AA7075

to define ferrite and austenite grains and to observe dislocations (what kind of dislocations they are and where are they located in the specimens). An example of accumulation of dislocations at the grain boundary between ferrite and austenite in DSS aged specimen (annealed at 350 °C for 30 000 h) is shown in **Figure 7**. Spinodal decomposition is expected to occur during thermal ageing of this type of material. The characteristic is formation of nano-cellular microstructure of ferrite domains with regions enriched with Cr and other alphasene alloying elements as well as regions enriched with Co, N and other gammagene alloying elements. Because of difference in local chemical composition, lattice parameters are changed and their accommodation creates elastic stresses that increase the hardness and change mechanical properties (tensile strength increase, while ductility and toughness decrease). The change of mechanical properties may be related also to changes of material's internal structure (stacking faults, morphology and density of dislocations). It has been established that density of dislocations increased after ageing at 300 °C and that they appeared in different configurations with many of them being substantially mobile (numerous

side-trails and traces of dislocations escape to the foil surface). The dislocation configurations changed and many of dislocations became immobilized (or at least slowed down in their movements) after ageing at 350 °C when the transformation of the matrix occurred and achieved a virtually equilibrium state according to the effect of ageing temperature on the change of Charpy notch sharpness. Further investigations (TEM/EDXS) will enable to better understand the characteristics of spinodal decomposition, the influence of ferrite presence in DSS and thus help to increase the life-time of components of thermal power plants including elements of DSS. They will enable to explain the real rearrangement of alloying elements and formation of eventual new phases during spinodal decomposition as well.

3.2.4 Investigation of precipitates in AA7075 aluminium alloy

AA7075 aluminium alloy is used for automotive components such as pistons, rocker arms, brake callipers and wheels, as well as application in various fields of sport, electronic and aerospace industry. The properties of this alloy are strongly affected by heat treatments,

which change the microstructure of the alloy to achieve optimum mechanical properties.³⁶ Within this alloy the large population of intermetallic particles cause a problem of severe localised corrosion due to strong galvanic coupling within the matrix. The intermetallics are formed by the interaction between alloying elements and impurities present in the alloy and may be phases largely based upon the principal alloying elements (Zn and Mg) and can undergo phase transformation and change of morphology during homogenization of alloys, but they are insoluble during solution heat treatment at lower temperature and subsequent ageing.

Specimens of AA7075 aluminium alloy were homogenized at 460 °C for 6 h and air quenched. The TEM was used to assess the shape and size of different precipitates (**Figure 8**) and to determine their chemical composition. Areas of thin foils rich in precipitates were analyzed by means of EDXS. Precipitates differed by morphology, size and contrast. The matrix consisted of bigger rods of about 10³ nm long and up to 100 nm thick, and of smaller rods also, that differed in composition from the bigger rods. A large number of smaller precipitates of polygonal shapes were present, too. By means of EDXS it was determined that bigger rods consisted of magnesium, aluminium, copper and zinc, while smaller rods contained, apart these elements, also chromium. Polygonal shaped precipitates differed mutually also by contrast. Some contained magnesium, aluminium, copper and zinc but in different ratios as in bigger rods. Other contained aluminium, chromium, copper, zinc, nickel, iron and manganese. The detailed results of this study will be the object of a new article.

4 CONCLUSIONS

The capabilities of high-resolution transmission electron microscope JEOL JEM-2100 with a conventional high brightness LaB₆ electron source allow it effective use in most of routine structure studies of nano-materials. Nanoparticles as small as 5–10 nm can be easily and unambiguously identified by Fourier analysis of high-resolution images combined with elemental X-ray microanalysis or STEM image observation device, coupled with elemental mapping or line profiling techniques. This is demonstrated through several examples of investigations that were carried out at the Institute of Metals and Technology in Ljubljana.

Acknowledgments

This work has been supported by the research program "Surface physics and chemistry of metallic materials" P2-0132 and by the "Physics and chemistry of porous aluminium for Al panels capable of highly efficiently energy absorption" project L2-2410 (D), funded by the Slovenian Research Agency. The author wishes to thank M. Jenko, B. Šuštaršič, B. Marini

(CEA), M. Godec, Č. Donik, P. Cvahte (Impol), and I. Paulin for their cooperation and for providing the specimens. Thanks also to M. Pečar, S. Žižek (Scan), R. Ravelle - Chapuis (JEOL Europe SAS) and S. Asahina (JEOL Europe SAS) for valuable advice with TEM operations and thin foil specimen preparations.

5 REFERENCES

- Available from World Wide Web: <http://www.nano.gov/html/facts/whatIsNano.html>
- D. Jenko, A. Benčan, B. Malič, J. Holc, M. Kosec, *Microsc. Microanal.*, 11 (2005) 6, 572–580
- A. Benčan, E. Tchernychova, M. Godec, J. G. Fisher, M. Kosec, *Microsc. Microanal.*, 15 (2009) 5, 435–440
- D. A. Skobir, M. Godec, M. Jenko, B. Markoli, *Surface and Interface Analysis*, 40 (2008) 3/4, 513–517
- D. A. Skobir, F. Vodopivec, S. Spaic, B. Markoli, *Zeitschrift Fur Metallkunde*, 95 (2004) 11, 1020–1024
- M. Remskar, A. Mrzel, M. Virsek, M. Godec, M. Krause, A. Kolitsch, A. Singh, A. Seabaugh, *Nanoscale research letters*, 6 (2011), article number 26, doi: 10.1007/s11671-010-975-0
- D. Mandrino, M. Godec, M. Torkar, M. Jenko, *Surface and Interface Analysis*, 40 (2008), 3/4, 285–289
- M. Torkar, M. Godec, M. Lamut, *Engineering Failure Analysis*, 14 (2007) 7, 1218–1223
- M. Godec, D. Nolan, M. Jenko, *Materials science & engineering B, Solid-state materials for advanced technology*, B 129 (2006) 1, 31–38
- M. Godec, D. Mandrino, M. Jenko, *Engineering Failure Analysis*, 16 (2009) 4, 1252–1261
- M. Godec, A. Kocijan, D. Dolinar, D. Mandrino, M. Jenko, V. Antolič, *Biomedical Materials*, 5 (2010) 4, doi: 10.1088/1748-6041/5/4/045012
- M. Jenko, F. Vodopivec, H. J. Grabke, H. Viehhaus, B. Praček, M. Lucas, M. Godec, *Steel Research*, 65 (1994) 11, 500–504
- M. Jenko, F. Vodopivec, B. Praček, M. Godec, D. Steiner, *Journal of Magnetism and Magnetic Materials*, 133 (1994) 1–3, 229–232
- M. Jenko, B. Korosic, D. Mandrino, V. Presern, *Vacuum*, 57 (2000) 3, 295–305
- D. Mandrino, D. Vrbanic, M. Jenko, D. Mihailovic, S. Pejovnik, *Surface and Interface Analysis*, 40 (2008) 9, 1289–1293
- D. Mandrino, M. Godec, M. Torkar, M. Jenko, *Surface and Interface Analysis*, 40 (2008) 3–4, 285–289
- B. S. Batic, M. Jenko, *Journal of Vacuum Science & Technology A, Vac. surf. films*, 28 (2010) 4, 741–744
- B. S. Batic, M. Jenko, *Surface and Interface Analysis*, 42 (2010) 6–7, 703–706
- A. Minovič, I. Milošev, V. Pišot, A. Cör, V. Antolič, *J. bone jt. surg.*, 83-B (2001) 8, 1182–1190
- A. Kocijan, M. Conradi, *Mater. Tehnol.*, 44 (2010), 1, 21–24
- A. Kocijan, D. K. Merl, M. Jenko, *Corrosion Science*, 53 (2011) 2, 776–783
- V. Leskovšek, B. Podgornik, M. Jenko, *Wear*, 266 (2009) 3/4, 453–460
- D. A. Skobir, M. Jenko, D. Mandrino, *Surface and Interface Analysis*, 36 (2004) 8, 941–944
- J. Vojvodič-Tuma, B. Šuštaršič, R. Celin, F. Vodopivec, *Mater. Tehnol.*, 43 (2009) 4, 179–187
- J. Vojvodič-Tuma, B. Šuštaršič, F. Vodopivec, *Nucl. Eng. Des.*, 238 (2008) 7, 1511–1517
- D. B. Williams, C. B. Carter, *Transmission Electron Microscopy: A Textbook for Materials Science*, 2nd ed., Springer, New York 2009, pp. 832

- ²⁷ J. Ayache, L. Beaunier, J. Boumendil, G. Ehret, D. Laub, *Sample Preparation Handbook for Transmission Electron Microscopy: Methodology*, Springer, New York 2010, pp. 250
- ²⁸ J. Ayache, L. Beaunier, J. Boumendil, G. Ehret, D. Laub, *Sample Preparation Handbook for Transmission Electron Microscopy: Techniques*, Springer, New York 2010, pp. 338
- ²⁹ R. M. Anderson, S. D. Walck, *Specimen Preparation for Transmission Electron Microscopy of Materials IV*, Materials Research Society Symposium Proceedings Volume 480, San Francisco, **1997**, 295
- ³⁰ I. Paulin, B. Sustarsic, V. Kevorkijan, S. D. Skapin, M. Jenko, *Mater. Tehnol.*, 45 (**2011**) 1, 13–19
- ³¹ I. Paulin, D. Mandrino, C. Donik, M. Jenko, *Mater. Tehnol.*, 44 (**2010**) 2, 73–76
- ³² V. Kevorkijan, S. D. Skapin, I. Paulin, B. Sustarsic, M. Jenko, *Mater. Tehnol.*, 44 (**2010**) 6, 363–371
- ³³ C. Donik, A. Kocijan, D. Mandrino, I. Paulin, M. Jenko, B. Pihlar, *Applied Surface Science*, 255 (**2009**) 15, 7056–7061
- ³⁴ C. Donik, A. Kocijan, J. T. Grant, M. Jenko, A. Drenik, B. Pihlar, *Corrosion Science*, 51(**2009**) 4, 827-832
- ³⁵ C. Donik, D. Mandrino, M. Jenko, *Vacuum*, 84 (**2010**) 11, 1266–1269
- ³⁶ F. Andreatta, H. Terryn, J. H. W. de Wit, *Electrochimica Acta*, 49 (**2004**), 2851–2862